

Research Article

A New Method for Estimating Dermal Absorption from Chemical Exposure. 1. General Approach

Robert L. Cleek¹ and Annette L. Bunge^{1,2}

Received April 4, 1992; accepted October 4, 1992

To evaluate systemic chemical exposure from dermal absorption, one must know the mass of chemical absorbed including the portion that has entered the skin but not yet entered the body's interior system. Algebraic equations are presented for estimating dermal absorption including the effects of exposure time and chemical nature of the compound, in particular lipophilicity and molecular weight. The proposed equations account for larger absorption rates during the initial exposure period as well as the hydrophilic barrier which the viable epidermis presents to lipophilic chemicals. These algebraic expressions are shown to represent adequately the exact solution of the unsteady-state diffusion equations for a two-membrane composite. Finally, procedures are proposed for estimating a priori the required physicochemical data when experimental values are not available. Specifically, the Potts and Guy permeability correlation is split into parts separately representing stratum corneum partitioning and diffusivity.

KEY WORDS: dermal absorption; exposure assessment; percutaneous absorption; mathematical models.

INTRODUCTION

Estimates of human health risk must account for all routes of exposure including dermal absorption. Some risk assessments have assumed a fixed percentage of the dermal exposed dose is absorbed (1-3) based on human or animal experiments or arbitrarily chosen as 100% to provide the most conservative estimate of risk. Such approaches are inconsistent with extensive research of dermal penetration which has established that the amount absorbed is a function of the exposure time and the chemistry of the compound, in particular its lipophilicity and molecular weight (4-6).

Figure 1 illustrates the effect of exposure time on the mass absorbed into the stratum corneum (SC) and leaving from the SC to enter the body's interior system, assuming that the concentration of chemical on the SC surface (C_v^o) remains constant. The cumulative mass in and out of the SC is normalized by C_v^o and the SC-vehicle partition coefficient (K_{cv}), permitting all chemicals to be presented on an equal basis. At a given time, the difference between the in and the out curves represents the mass residing in the SC. *In vitro* and *in vivo* experiments have established the validity of these calculated results (7-15).

Absorption is more rapid during the unsteady period preceding the lag time (t_{lag}), when chemical primarily fills the SC reservoir and almost no mass leaves the SC. Some time after t_{lag} , steady state is reached and the rates at which mass enters into and leaves from the SC are equal and constant.

Quantitative estimates for t_{lag} are usually obtained by extrapolating the linear (i.e., steady-state) portion of the cumulative mass out curve to zero (Fig. 1).

The total mass absorbed into the SC during the exposure event includes chemical that has entered but not yet left the SC. After the exposure event ends, chemical continues to diffuse from the SC to enter the body's interior system. In practice, especially for highly lipophilic chemicals, the time required to move from the SC into the system may be quite long and some of the absorbed chemical may be removed by metabolism, washing, desquamation, or evaporation before diffusion into the interior system is complete. However, with almost no information on these removal processes, risk assessments should be based on estimates of the total mass absorbed into the SC. Estimating dermal exposure with methods predicting the mass flux out of the SC will greatly underrepresent the potential risk.

Some risk assessors have proposed calculating the amount absorbed using the steady-state permeability from a given vehicle (P_v) multiplied by the area of exposure, the absorbing chemical's concentration in the vehicle (C_v^o), and the time of the exposure event (t_{exp}). That is,

$$M = P_v A C_v^o t_{exp} \quad (1)$$

Although appealingly simple, this approach also underestimates the mass absorbed as indicated by the line designated steady state in Fig. 1. In some cases such as showering or bathing, exposure events may be relatively short, meaning that steady state is never reached. Even when exposures are long enough for steady state to be achieved, the mass absorbed during the unsteady-state period must be included in

¹ Chemical Engineering and Petroleum Refining Department, Colorado School of Mines, Golden, Colorado 80401.

² To whom correspondence should be addressed.

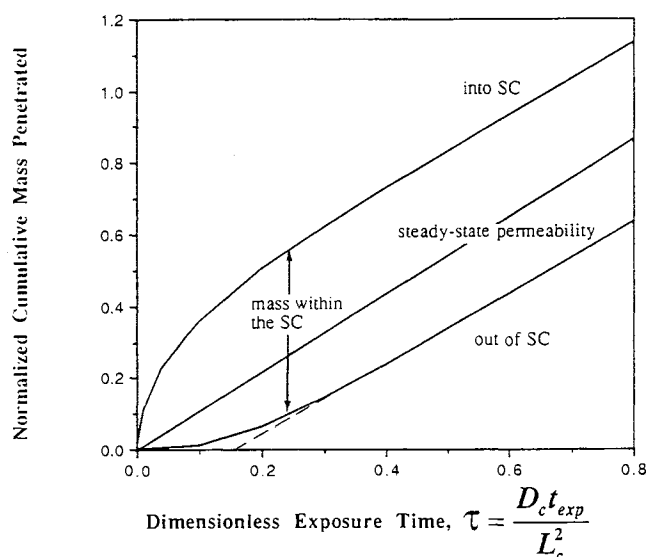


Fig. 1. Cumulative mass of chemical penetrating into and out of the stratum corneum normalized by $(AL_c K_{cv} C_v^0)$ as a function of dimensionless t_{exp} .

the estimate. Consequently, absorption during the unsteady-state period is always important regardless of the time of exposure.

BACKGROUND

The rate at which a chemical absorbs into the SC depends on both its lipophilic character and its molecular weight (MW). Based on a large data base of steady state *in vitro* permeability experiments from a water vehicle, Potts and Guy (6) have shown that the steady-state SC permeability from water (P_{cw}) can be reasonably represented by

$$\log P_{cw} \text{ (cm/hr)} = -2.8(\pm 0.08) - 6.0(\pm 0.6) (10^{-3}) (\text{MW}) + 0.74(\pm 0.07) \log K_{ow} \quad (2)$$

where K_{ow} is the octanol-water partition coefficient and the coefficients are indicated with standard deviations derived from a multiple regression analysis. Hence, compounds with larger K_{ow} have larger SC permeabilities provided that their molecular weights (MW) are not too much larger.

Equation (2) was developed from data compiled by Flynn (5) of over 90 compounds, ranging in MW from 18 to 750 and in $\log K_{ow}$ from -3 to 6, with a high level of statistical significance ($r^2 = 0.67$). It is generally observed that experimental variation in human skin permeability is about 30% (16). The fact that Eq. (2) is able to represent about 70% of the variability in this large body of data is a rigorous test of the model. Furthermore, Eq. (2) averages most of the experimental variability. Consequently, when differences arise between Eq. (2) and experimental permeabilities, the weight of the experimental data strongly supports the validity of the correlation prediction. While experimental results must be carefully considered, data which deviate significantly from Eq. (2) should be evaluated critically for experimental procedure and reproducibility before such data are accepted as more representative than the correlation. According to Potts and Guy (6), experimental results which

vary from Eq. (2) by a factor of more than about 3 would lie outside of the 95% confidence interval.

A correlation such as Eq. (2) has been derived from about 20 compounds permeating hairless mouse skin (17). The coefficient multiplying MW is significantly smaller for hairless mouse than for human skin, while differences in all other coefficients are small and statistically insignificant. Consequently, permeability values for hairless mouse skin are less sensitive to increases in MW than is human skin, and the ratio of permeabilities from hairless mouse and human skin will vary with MW. The MW dependence of other animal skins will probably be different also, suggesting that errors from using animal skins to represent human skin will vary with MW.

The steady-state permeability across the SC from a vehicle v (P_{cv}) into an infinite sink depends on the diffusivity of the chemical in the SC (D_c), the SC thickness (L_c), and the equilibrium partition coefficient between the SC and the vehicle (K_{cv}) as given below:

$$P_{cv} = K_{cv} D_c / L_c \quad (3)$$

where K_{cv} is defined as the concentration of chemical in the SC (mass/volume of SC at absorbing conditions) divided by the equilibrium concentration in the vehicle (mass/volume) (13). As defined here, D_c is an effective diffusivity based on the SC thickness rather than the true diffusivity based on the actual molecular diffusion path length, which is not known.

The barrier resistance provided by the SC is $1/P_{cv}$. However, for intact skin the barrier includes the viable epidermis (EPI) in addition to the SC, and the steady-state resistance ($1/P_v$) is the sum of these two resistances:

$$\frac{1}{P_v} = \frac{1}{P_{cv}} + \frac{1}{P_{ev}} \quad (4)$$

where steady-state permeability through the EPI from a vehicle v is defined as

$$P_{ev} = K_{ev} D_e / L_e \quad (5)$$

K_{ev} is the EPI-vehicle partition coefficient, and D_e and L_e are the diffusivity of chemical in and thickness of the EPI, respectively. If the vehicle itself does not alter the thermodynamic character of the SC or EPI,

$$K_{ev} = K_{cv} / K_{ce} \quad (6)$$

and the resistance of the SC-EPI composite barrier is then

$$\frac{1}{P_v} = \frac{1}{P_{cv}} \left[1 + \frac{K_{ce} D_c L_e}{D_e L_c} \right] = \frac{1}{P_{cv}} (1 + B) \quad (7)$$

where the parameter B , defined as

$$B = \frac{D_c L_e K_{ce}}{D_e L_c} = \frac{P_{cv}}{P_{ev}} \quad (8)$$

measures the relative permeability of the SC to the EPI and is independent of the vehicle, provided that the vehicle has not altered physicochemically the SC or EPI. Hence, B values from one vehicle, such as water, can be used in calculations for other vehicles.

Because diffusivity in the EPI is much larger than in the SC, B is often small and the permeability across the SC-EPI

barrier nearly equals the permeability of the SC alone. The EPI is much more hydrophilic than the SC and K_{ce} will be similar to partitioning between lipophilic and hydrophilic solvents, such as octanol and water. Consequently, chemicals with large K_{ow} will have large values for B , indicating that the resistance across the EPI ($1/P_{ev}$) is larger than the resistance across the SC ($1/P_{cv}$). When B is large, the total permeability of the combined SC-EPI barrier no longer depends solely on the SC permeability. These highly lipophilic compounds enter the relatively hydrophilic EPI with difficulty, thereby causing the total permeability of the combined SC-EPI barrier to be less than the permeability across only the SC. Since many chemicals of environmental interest are highly lipophilic, dermal absorption estimates should include effects of the SC-EPI combined barrier.

THEORY

We have developed a set of algebraic equations which accurately represents dermal absorption including unsteady-state contributions and the EPI resistance to highly lipophilic compounds. Three mathematical absorption models provide important insights in the development and testing of these algebraic expressions: a single finite membrane, a semiinfinite membrane, and a finite two-membrane composite.

All three models assume that the membranes (SC or SC/EPI) are passive with constant diffusivities, thicknesses, and partition coefficients. That is, the vehicle and the absorbing chemical do not alter these properties. Although the SC and EPI are both heterogeneous membranes, mathematically we treat them as pseudohomogeneous, an approach supported by research on both skin and other synthetic membranes (18–20). As a consequence, the diffusivity, thickness, and partition coefficient values are effective properties. We assumed that a constant vehicle concentration (C_v^0) instantaneously equilibrates with the outer layer of the SC, that the initial chemical concentration in the skin layers is zero, and that the chemical concentration in the body system remains zero during the entire exposure event. The cumulative mass absorbed into the SC per unit area of exposure (M_{in}/A) is found by integrating the mass flux across the exposed SC surface during the time of exposure.

All three models discussed here have been described previously for various applications by many authors (e.g., see Refs. 20–22), sometimes with small variations. Consequently, the solutions presented here are not new, but included as necessary justification for the proposed system of algebraic expressions approximating dermal absorption, which is new. A complete description of the corresponding differential equations, restricting conditions, and analytical solutions is given elsewhere (23).

Single Finite Membrane

Figure 2 schematically depicts the SC as a single finite membrane of thickness L_c . The normalized cumulative mass absorbed into the SC, $M_{in}/(AL_cK_{cv}C_v^0)$ is

$$\frac{M_{in}}{AL_cK_{cv}C_v^0} = \tau + \frac{1}{3} - \frac{2}{\pi^2} \sum_{n=1}^{\infty} \frac{e^{-n^2\pi^2\tau}}{n^2} \quad (9)$$

where

$$\tau = \frac{t_{exp}D_c}{L_c^2} \quad (10)$$

is the exposure time t_{exp} normalized by the characteristic diffusion time (L_c^2/D_c) for a chemical in the SC. The normalized cumulative mass out of the SC is calculated by integrating the flux at L_c over the exposure time:

$$\frac{M_{out}}{AL_cK_{cv}C_v^0} = \tau - \frac{1}{6} - \frac{2}{\pi^2} \sum_{n=1}^{\infty} \frac{(-1)^n e^{-n^2\pi^2\tau}}{n^2} \quad (11)$$

The results from Eqs. (9) and (11) were used to calculate the curves shown in Fig. 1. The infinite series in Eq. (9) makes this equation inconvenient to use for routine calculations, especially for shorter exposure times.

For long exposure times, Eqs. (9) and (11) simplify to give expressions for the normalized cumulative mass M^∞ in and out of the SC:

$$\frac{M_{in}^\infty}{AL_cK_{cv}C_v^0} = \tau + 1/3 \quad (12)$$

$$\frac{M_{out}^\infty}{AL_cK_{cv}C_v^0} = \tau - 1/6 \quad (13)$$

Equation (13) mathematically represents the linear, long-time portion of the normalized cumulative mass-out curve in Fig. 1. Extrapolation of this line to zero cumulative mass defines the dimensionless lag time ($t_{lag}D_c/L_c^2$), which is 1/6. Importantly, t_{lag} is independent of K_{cv} . Chemicals with different K_{cv} as indicated by different K_{ow} can still exhibit similar t_{lag} provided that their D_c values are comparable. Reproducible experimental values for t_{lag} can be difficult to obtain (13,19), especially for lower molecular weight chemicals with larger D_c . However, when the SC is the primary mass transfer barrier and reliable t_{lag} data are available, dimensionless exposure times can be calculated as $\tau = t_{exp}/6t_{lag}$.

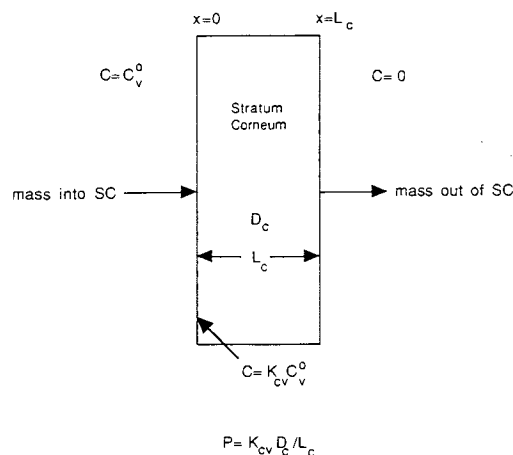


Fig. 2. Schematic diagram of permeation into and across only the stratum corneum.

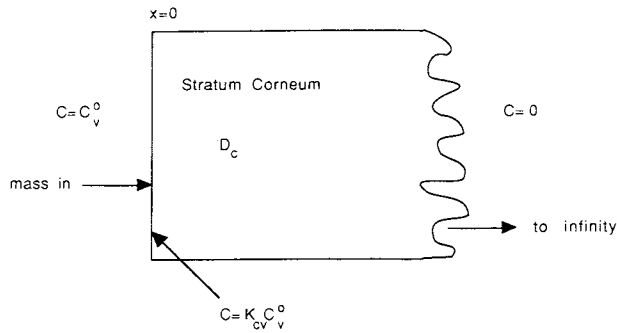


Fig. 3. Schematic diagram of permeation into a semi-infinite stratum corneum.

Semi-Infinite Membrane

When t_{exp} is small, the chemical will penetrate only a short distance into the SC. In this situation, the SC will seem to be very thick, or semi-infinite, as illustrated in Fig. 3. The normalized cumulative mass absorbed is then given by the well-known expression

$$\frac{M_{in}}{AL_c K_{cv} C_v^0} = 2 \sqrt{\frac{D_c t_{exp}}{L_c^2 \pi}} = 2 \sqrt{\frac{\tau}{\pi}} \quad (14)$$

which predicts that the cumulative mass absorbed varies with the square root of time.

Finite Two-Membrane Composite

Figure 4 illustrates a more realistic picture for dermal exposure which includes both the SC and the EPI layers. We assume that the SC-EPI interface instantaneously equilibrates. That is, the concentrations in the SC and EPI at the SC-EPI interface are related by the partition coefficient between the two layers (K_{ce}). Furthermore, we assume that partition coefficients between the vehicle and the SC and EPI, respectively, are related as given in Eq. (6). In this case, the normalized cumulative mass absorbed into the SC is given by

$$\begin{aligned} \frac{M_{in}}{AL_c K_{cv} C_v^0} = & \frac{1}{1+B} \left[\tau + \frac{G(1+3B) + B(1+3BG)}{3G(1+B)} \right. \\ & + 2(1+B) \sum_{n=1}^{\infty} \frac{\sin(\lambda_n/\sqrt{G}) \sin(\lambda_n) \exp(-\lambda_n^2 \tau)}{\lambda_n^2 \sigma_n} \\ & \left. - 2(1+B) \sum_{n=1}^{\infty} \frac{\cos(\lambda_n/\sqrt{G}) \cos(\lambda_n) \exp(-\lambda_n^2 \tau)}{B\sqrt{G}\lambda_n^2 \sigma_n} \right] \quad (15) \end{aligned}$$

where σ_n are

$$\begin{aligned} \sigma_n = & \frac{1}{BG} [\sqrt{G}(1+B) \cos(\lambda_n/\sqrt{G}) \cos(\lambda_n) \\ & - (1+GB) \sin(\lambda_n/\sqrt{G}) \sin(\lambda_n)] \quad (16) \end{aligned}$$

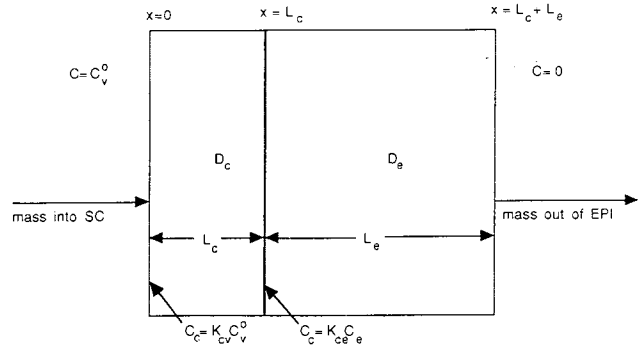


Fig. 4. Schematic diagram of permeation into and across the stratum corneum and viable epidermis.

and λ_n are eigenvalues specified by

$$\sqrt{GB} \tan(\lambda_n/\sqrt{G}) + \tan(\lambda_n) = 0 \quad (17)$$

which are found by trial and error. The parameter G , defined as

$$G = \frac{L_c^2 D_e}{L_e^2 D_c} \quad (18)$$

is the ratio of the SC and EPI lag times. The parameter B measures the relative contribution of the EPI and SC resistances [Eq. (8)].

RESULTS AND DISCUSSION

Unsteady-State Absorption into a Single Membrane

Figure 5 compares the normalized cumulative mass absorbed into the SC as a function of dimensionless t_{exp} (τ) when the SC is semi-infinite and finite, as calculated from Eqs. (9) and (14), respectively. The normalized cumulative mass absorbed for chemicals with different K_{cv} or C_v^0 is the

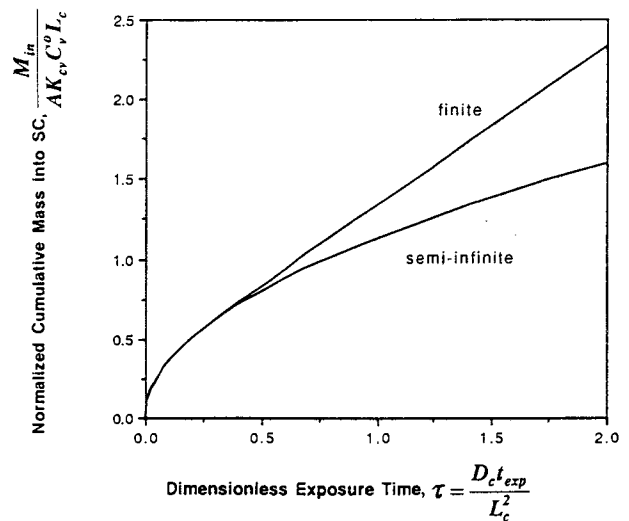


Fig. 5. Comparing predictions of the normalized cumulative mass absorbed into the stratum corneum [$M_{in}/(AL_c K_{cv} C_v^0)$] modeled as a finite single membrane and a semi-infinite membrane.

same when compared at the same τ . To calculate the actual cumulative mass absorbed one multiplies the normalized cumulative mass by $(AL_c K_{cv} C_v^0)$. For example, if $(K_{cv} C_v^0)$ for chemical A is 10 times larger than for chemical B, the cumulative mass absorbed during the same dimensionless exposure time τ will be 10 times larger for chemical A than for chemical B.

Absorption into the finite SC eventually reaches steady state as indicated by the constant slope for larger τ . In contrast, the absorption rate for a semi-infinite SC continues to decline with longer exposure times as the chemical is forced to penetrate further into the SC. Notice that the exposure time, t_{exp} , required to reach steady state will be longer for chemicals with smaller D_c .

Not surprisingly, Eqs. (9) and (14) give identical results during shorter t_{exp} . That is, the chemical does not penetrate far enough in this time to see that the SC has a finite thickness. Consequently, the computationally simpler semi-infinite membrane expression, Eq. (14), describes absorption into the SC during the unsteady-state period.

Absorption into a Finite Two-Membrane Composite

Figure 6 shows the normalized cumulative mass of chemical absorbed as a function of dimensionless t_{exp} and B for the SC-EPI composite membrane as described by Eq. (15) when G is 10 or larger. During the unsteady-state period, the normalized cumulative mass absorbed into the SC is independent of B and G . For unsteady-state exposure times, the chemical has only penetrated the SC and is not yet affected by the EPI. Consequently, the semi-infinite membrane, Eq. (14), can be used to predict unsteady-state absorption regardless of a chemical's lipophilic character. We emphasize that it is the normalized cumulative mass ($M_{in}/AK_{cv}C_v^0L_c$) and not the actual cumulative mass absorbed (M_{in}), which is independent of the chemical's lipophilic character.

For longer times, the normalized cumulative mass absorbed into the SC becomes linear with time (as steady state

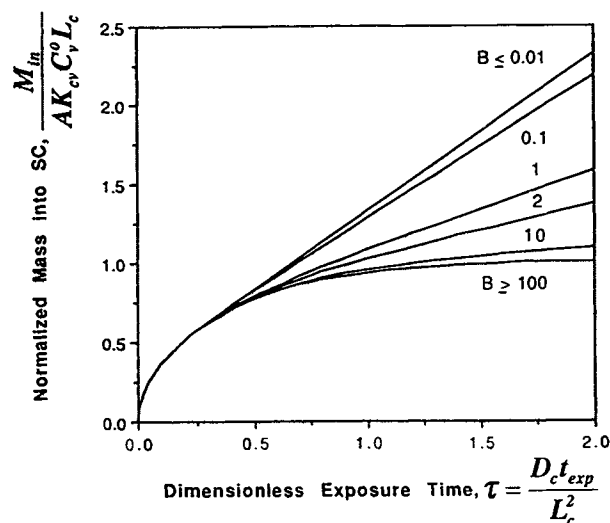


Fig. 6. Normalized cumulative mass entering the stratum corneum [$M_{in}/(AL_c K_{cv} C_v^0)$] as a function of dimensionless t_{exp} when the viable epidermis is present.

is reached) and decreases as the lipophilicity increases (i.e., B increases). The relatively hydrophilic EPI chokes the flux of highly lipophilic chemicals from the SC, which in turn restricts the flux of chemical entering into the SC. Limiting conditions are reached for either highly lipophilic compounds ($B > 100$) or relatively hydrophilic compounds ($B < 0.01$).

The steady-state cumulative mass absorption is found by simplifying Eq. (15) for long t_{exp} to give (31,32)

$$\frac{M_{in}}{AL_c K_{cv} C_v^0} = \frac{1}{1+B} \left[\tau + \frac{G(1+3B) + B(1+3BG)}{3G(1+B)} \right] \quad (19)$$

For large values of G , Eq. (19) further simplifies to

$$\frac{M_{in}}{AL_c K_{cv} C_v^0} = \frac{1}{1+B} \left[\tau + \frac{1+3B+3B^2}{3(1+B)} \right] \quad (20)$$

which no longer depends on G . Calculations described elsewhere (30) show that Eq. (20) is accurate when G is larger than 10, which is the case as long as the SC is not compromised by damage or extremely effective enhancers.

As indicated in Eq. (20), the steady-state slope of the normalized cumulative mass absorbed is $1/(1+B)$, which corresponds to P_v/P_{cv} as specified in Eq. (7). For highly lipophilic compounds ($B > 100$), the slope of the steady-state portion of the cumulative mass curve approaches zero. For more hydrophilic compounds ($B < 0.01$), the slope of the steady-state cumulative mass curve approaches the permeability of the SC alone.

The intercept of Eq. (20) on the normalized cumulative mass axis increases as the lipophilicity of the absorbing chemical increases to reach a maximum of one. If the EPI is a total barrier to dermal absorption (i.e., infinitely large B), the SC eventually would become entirely equilibrated with the given vehicle concentration, C_v^0 . In this case, the normalized cumulative mass absorbed approaches one, corresponding to the amount required to saturate the stratum corneum completely. When B is small, the SC permeability will control the amount absorbed and the intercept of the steady-state line predicted by Eq. (20) is $1/3$, consistent with the long t_{exp} limit of the single finite membrane case, Eq. (12).

We can approximately represent the curves in Fig. 6 using Eq. (14) for the unsteady-state period ($t_{exp} \leq t^*$) followed by Eq. (20) for longer exposure times ($t_{exp} > t^*$). We determine the transition time, t^* , by minimizing the difference between the actual mass absorbed, calculated from Eq. (15), and the approximate mass absorbed, calculated from Eqs. (14) and (20).

When $B \geq 0.6$, a good value for t^* is t_{exp} when Eqs. (14) and (20) intersect. When B is smaller than 0.6, Eqs. (14) and (20) do not intersect for any t_{exp} , but the minimum error occurs when t^* is $0.4 L_c^2/D_c$. This value for t^* compares well with Crank's (20) conclusion that steady-state absorption across a single membrane is reached when t_{exp} is about $0.45 L_c^2/D_c$. Recommended values for t^* are given in Table I.

The transition time t^* essentially represents the t_{exp} required to reach steady state. As such, t^* is always larger than t_{lag} and depends on whether the SC, the EPI, or both the SC and the EPI contribute significantly to the barrier's resistance. For example, when the SC controls absorption ($B \leq$

0.1), t^* is $2.4 t_{lag}$. When the EPI controls absorption ($B \gg 100$), $t^* D_c/L_c^2$ is about 0.8, corresponding to $4.8 t_{lag}$ if t_{lag} is defined as $D_c/6L_c^2$.

Estimating Dermal Absorption

Table I summarizes the set of algebraic equations proposed to predict the cumulative mass absorbed into the SC during an exposure event. In the case of multiple exposures, we suggest assuming that the SC is completely void of chemical prior to each new exposure to provide an estimate of the maximum possible absorption. Because the equations in Table I assume a constant concentration during the exposure event, when chemical is depleted by absorption or evaporation, these estimates will be larger than the actual amount absorbed. However, nonvolatile liquid or oily chemicals which are dissolved in volatile vehicles are exceptional cases with potentially larger amounts of absorption than predicted by the method proposed here.

Figure 7 illustrates the differences between the complete unsteady-state SC-EPI composite membrane expression, Eq. (15), and estimates made using the equations from Table I for three values of B . Figure 8 shows the percentage relative error between the exact and the estimated expressions as a function of dimensionless exposure times for B values greater than 100 and less than 0.01. The discontinuities in the relative error curves occur at the transition from Eq. (14) to Eq. (20). Since these values of B represent limiting conditions for the cumulative mass absorbed into the SC (Fig. 6), the relative error between the exact amount absorbed and estimates made from equations in Table I is bounded by the curves in Fig. 8 and will never exceed approximately 13%. Errors are greatest for large values of B and t_{exp} near t^* .

Predictions of the normalized cumulative mass ab-

Table I. Summary of Equations for Estimating Dermal Absorption

$$B = P_{cw} \sqrt{MW} / 2.6, \quad P_{cw} = \frac{D_c K_{cw}}{L_c}$$

$$\log(K_{cw}) = 0.74 \log(K_{ow})$$

$$\log\left(\frac{D_c}{L_c}, \text{ cm/hr}\right) = -2.8 - 6.0(10^{-3})MW, \quad L_c = 10^{-3} \text{ cm}$$

$$\text{If } B \leq 0.6, \text{ then } t^* = \frac{0.4L_c^2}{D_c}$$

$$\text{If } B > 0.6, \text{ then } t^* = (b - \sqrt{b^2 - c^2})L_c^2/D_c$$

$$b = \frac{2(1+B)^2}{\pi} - c$$

$$c = \frac{1 + 3B + 3B^2}{3(1+B)}$$

$$\text{If } t_{exp} \leq t^*, \text{ then } \frac{M_{in}}{A} = 2C_v^0 K_{cv} \sqrt{\frac{D_c t_{exp}}{\pi}}$$

$$\text{If } t_{exp} > t^*, \text{ then } \frac{M_{in}}{A} = \frac{C_v^0 L_c K_{cv}}{1+B} \left[\frac{D_c t_{exp}}{L_c^2} + \frac{1 + 3B + 3B^2}{3(1+B)} \right]$$

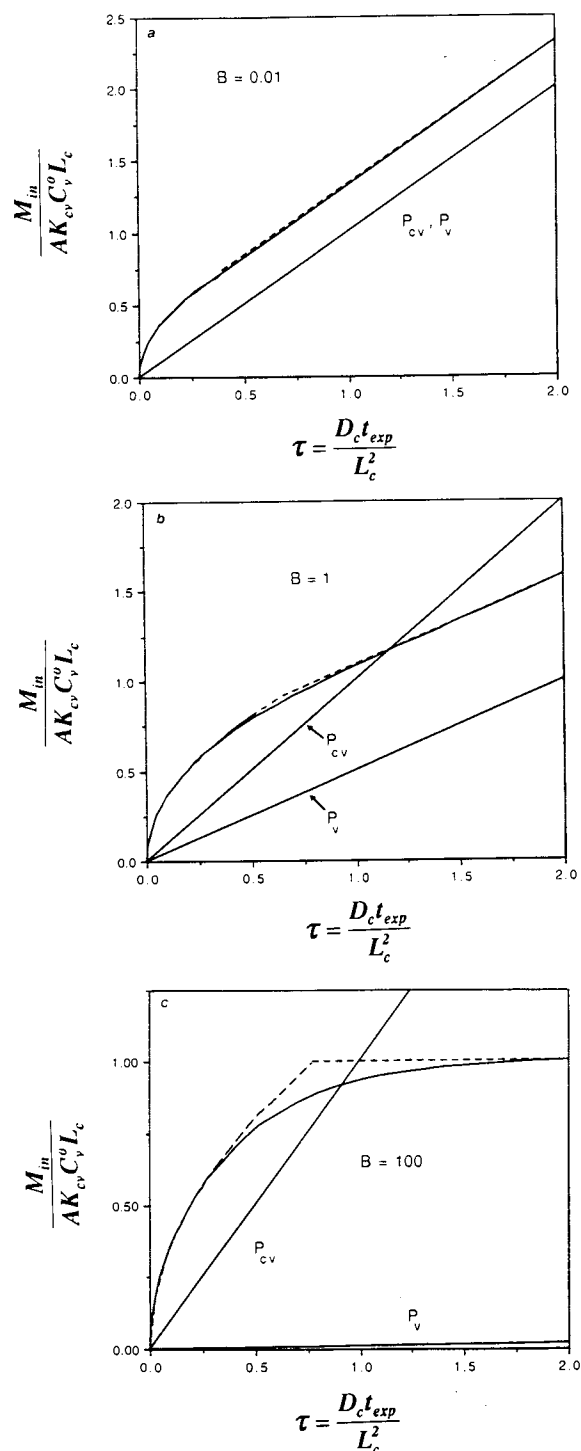


Fig. 7. Comparing predictions from the exact (solid), estimated (dashed), and steady-state (P_{cv} and P_v) expressions of the normalized cumulative mass absorbed into the stratum corneum [$M_{in}/(AL_c K_{cv} C_v^0)$] as a function of dimensionless t_{exp} $B =$ (a) 0.01, (b) 1, and (c) 100.

sorbed into the SC calculated from Eq. (1) are also included in Fig. 7. These calculations were made using the steady-state permeability for only the SC (P_{cv}) as well as the steady-state permeability for the SC-EPI composite membrane

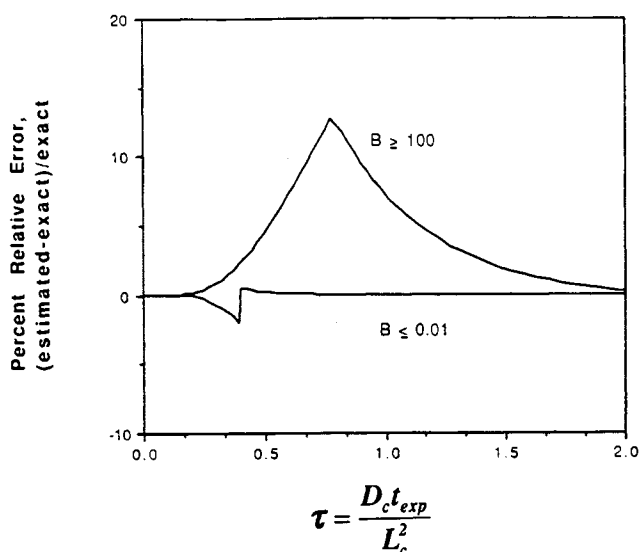


Fig. 8. Percentage relative error of the exact and estimated expressions for the cumulative mass absorbed into the stratum corneum as a function of dimensionless t_{exp} .

(P_v). Rewritten in terms of the normalized cumulative mass and including the definitions of P_{cv} and P_v from Eqs. (3) and (7), respectively, Eq. (1) reduces to

$$\frac{M}{AL_c C_v^0 K_{cv}} = \frac{\tau}{1 + B} \quad (21)$$

Equation (21) represents the normalized cumulative mass absorbed using the SC-EPI composite permeability, P_v . Assuming that B in Eq. (21) is zero provides an estimate of the normalized cumulative mass absorbed using the SC-only permeability, P_{cv} .

When B is small, the P_v and P_{cv} predictions are identical and underestimate the actual amount absorbed. For medium or high values of B , the P_v and P_{cv} predictions differ, with the P_v method always significantly underestimating the amount absorbed. As the permeability of the EPI-SC composite, P_v assumes that the additional resistance from the EPI always affects absorption. In fact, the presence of the EPI is not seen until the chemical has had time to diffuse through the SC. During this initial period, the absorption rates are controlled by the SC which is more permeable than the combined SC-EPI.

When the SC permeability, P_{cv} , is used in Eq. (1), the initial unsteady-state absorption is always underestimated. However, for more lipophilic chemicals with a significant mass transfer resistance in the EPI, P_{cv} will overestimate the amount absorbed at longer times (Figs. 7b and c). In this case, using P_{cv} in Eq. (1) does not correctly represent the additional resistance provided by the EPI.

Parameter Estimation

To use the equations in Table I requires estimates for L_c , D_c , K_{cv} , and B . The SC thickness varies with age, sex, and location on the body. However, 10–20 μm is a reasonable estimate for L_c (18).

Most experiments on human skin have measured the SC

or combined SC-EPI (and sometimes the dermis) permeability and not the separate components of permeability, D_c , and K_{cv} . As a first approximation, we divide the Potts and Guy correlation for steady-state SC permeability from water, Eq. (2), into parts separately representing D_c/L_c and K_{cw} as follows:

$$\log(D_c/L_c, \text{ cm/hr}) = -2.8 - 6.0 (10^{-3}) (MW) \quad (22)$$

$$\log K_{cw} = 0.74 \log K_{ow} \quad (23)$$

Consistent with its derivation, the SC-vehicle partition coefficient derived from Eq. (2) is for a water vehicle and is indicated as such in Eq. (23). Dermal absorption estimates using K_{cw} apply for absorption from aqueous solutions. Approaches for adjusting K_{cw} for calculations of absorption from nonaqueous vehicles are discussed elsewhere (24).

The division of Eq. (2) into parts separately representing the D_c/L_c and K_{cw} is supported by its semitheoretical development (6), as well as some SC-water partition coefficient experiments. The Scheuplein (25) data for normal alcohols and small undissociated acids from water correlate with K_{ow} when K_{ow} is not smaller than about 1.8 ($\log K_{ow} = -0.26$), corresponding to propanoic acid. A regression fit of the Scheuplein data (12 compounds with 3 to 8 carbons) yields

$$\log K_{cw} = -0.26(\pm 0.22) + 0.72(\pm 0.07) \log K_{ow} \quad (24)$$

with a correlation coefficient of 0.92. The values in parentheses indicate the standard error of the coefficients. Despite some data scatter, the highly hydrophilic compounds with $\log K_{ow} < -0.28$ (i.e., water, methanol, ethanol, formic acid, and acetic acid and indicated by triangles in Fig. 9) appear to reach a constant K_{cw} of about 0.9 ($\log K_{cw} = -0.065$).

In a more rigorous test, we derived a similar correlation for a larger data set consisting of K_{cw} for steroids (26) and phenolic compounds and aromatic alcohols (27) in addition to the Scheuplein data for normal alcohols and small acids. The resulting regression,

$$\log K_{cw} = -0.006(\pm 0.21) + 0.57(\pm 0.04) \log K_{ow} \quad (25)$$

with a correlation coefficient of 0.85 is indicated as the solid line in Fig. 9 and does not include the data represented by triangles. The dashed line in Fig. 9 corresponds to Eq. (23). Given the difficulties in acquiring reliable SC-partition coefficient data, the coefficients multiplying $\log K_{ow}$ in Eqs. (24) and (25) are essentially the same as in Eq. (23). This is encouraging evidence that the SC permeability of a chemical is affected primarily by its lipophilic character through only the partition coefficient.

The nonzero intercept of Eq. (24) differs from Eq. (23). However, given the limited amount of data on which Eq. (24) is based, the statistical significance of this nonzero intercept is small. In fact, a linear regression of the Scheuplein (25) data forcing a zero intercept gives:

$$\log K_{cw} = 0.60(\pm 0.04) \log K_{ow} \quad (26)$$

with a correlation coefficient of 0.85, which is nearly identical to Eq. (25). Differences in the coefficients multiplying the $\log K_{ow}$ term in Eqs. (23) and (25) are not statistically significant. Consequently, we choose Eq. (23) as a convenient and reasonable predictor for K_{cw} .

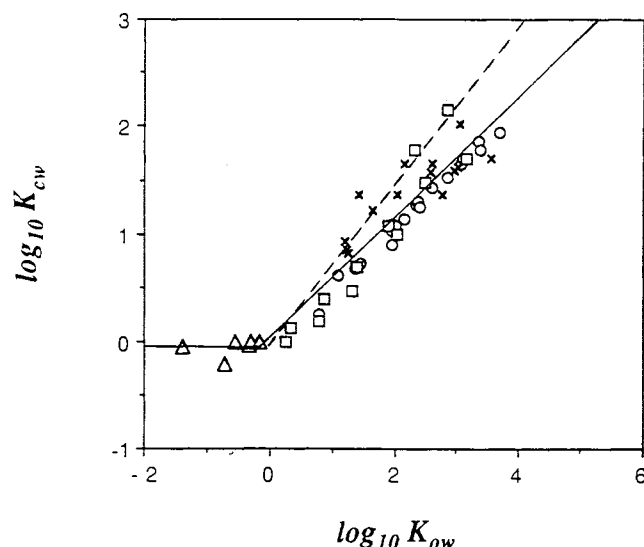


Fig. 9. K_{cw} as a function of K_{ow} for normal alcohols and undissociated acids (\square , Δ), steroids (\times), phenolic compounds and aromatic alcohols (\circ), Eq. 23 (---), and Eq. 25 (—).

As stated earlier, the Scheuplein (25) data suggest that Eq. (23) is not valid for chemicals with K_{ow} values smaller than 1.8 ($\log K_{ow}$ of -0.26). However, this limitation is not restrictive practically, since nearly all chemicals of interest for environmental exposures other than metals have $\log K_{ow}$ values larger than zero.

The failure of Eq. (23) to predict K_{cw} from $K_{ow} < 1.8$ contrasts with the success of Eq. (2) to predict steady-state permeabilities from water for $\log K_{ow}$ as low as about -3 . It may be that highly hydrophilic compounds partition significantly into the more polar keratin fraction of the SC, thereby exhibiting a larger than expected equilibrium SC-water partitioning which is insensitive to K_{ow} . At the same time, diffusion through the keratin fraction may be so much slower than diffusion through the lipids that the steady-state permeability reflects primarily transport through the lipids alone, resulting in a K_{ow} dependence even for the more hydrophilic chemicals. While these arguments are consistent with the observations, we note that the number of highly hydrophilic compounds for which K_{cw} are known are small, as is the number included in the data set regressed by Potts and Guy. Consequently a definitive answer to the apparent difference in the K_{ow} dependence for P_{cw} and K_{cw} requires more data for low- K_{ow} chemicals.

The time to reach steady-state t^* is a function of D_c/L_c^2 which depends on MW through Eq. (22). We can estimate the effect of MW by substituting Eq. (22) for D_c/L_c into the expressions given in Table I. Table II shows t^* values for compounds of various MW assuming a SC thickness of $10 \mu\text{m}$ and $B \leq 0.6$. If the SC is thicker than $10 \mu\text{m}$ or if the chemical is more lipophilic (i.e., $B > 0.6$), then the time to reach steady state will be even longer than the t^* values given in Table II. For chemicals with MW larger than 30, t^* is more than 20 min. Since all common pollutants listed by the U.S. EPA (28) have molecular weights exceeding 20, the unsteady-state Eq. (14) should predict the cumulative mass absorbed for t_{exp} of 20 min or less regardless of the chemical's K_{ow} .

Table II. Effect of Molecular Weight on t^* ^a

t^*	MW	D_c/L_c ($\times 10^4$ cm/hr)
20 min	20	12
26 min	50	7.9
1 hr	100	4.0
24 hr	330	0.17

^a Assumes $B < 0.1$. For $B > 0.1$, t^* will be larger.

As indicated in Eq. (8), B represents the ratio of the SC-to-EPI permeabilities, which in turn depend on the SC-to-EPI partition coefficient (K_{ce}) and the ratios of the SC-to-EPI diffusivities (D_c/D_e) and thicknesses (L_c/L_e). The parameter G also depends on D_c/D_e and L_c/L_e . Literature values reported for D_c/D_e and L_c/L_e are respectively 10^{-4} – 10^{-3} and between 5 and 10 (18). Consequently, G is always 10 or larger. For B calculations direct experimental values for K_{ce} do not exist, although a relationship between K_{ce} and K_{ow} is reasonable. Based on pharmacokinetic analysis of *in vivo* percutaneous absorption data, Guy and Hadgraft (29) infer that K_{ce} is approximately $K_{ow}/5$. Combining these values, B falls between $K_{ow}/10,000$ and $K_{ow}/500$.

Other functions of K_{ow} have been proposed or might be theoretically expected for K_{ce} . Furthermore, the SC-EPI diffusivity ratio may vary with MW. Depending on the values used for K_{ce} and D_c/D_e , quite different expressions for B result. Alternatively, the SC permeability, Eq. (2), can be used with an estimate of the EPI permeability. A more thorough discussion of approaches for estimating B and the impact on resulting dermal absorption predictions is discussed elsewhere, including example calculations for chemicals of environmental interest (30). Based on the discussions presented there, we recommend approximating B as

$$B = \frac{P_{cw} \sqrt{MW}}{2.6} \quad (27)$$

where P_{cw} (in cm/hr is estimated from Eq. (2)). Briefly, Eq. (27) assumes that the solubilizing character of the EPI is the same as water (i.e., $K_{cw} = 1$), P_{cw} is 10^{-4} cm/sec for chemicals with a MW of 50, and P_{cw} decreases as MW increases according to $1/\sqrt{MW}$.

CONCLUSIONS

Dermal absorption estimates should include the effects of time and chemical characteristics such as octanol-water partitioning and molecular weight. The cumulative mass adsorbed into the SC during t_{exp} should be used for assessing dermal exposure risks. Absorption calculations using the steady-state permeability, Eq. (1), always underestimate the mass of chemical absorbed into the SC during short exposure times (i.e., before reaching steady state). For highly lipophilic compounds ($\log K_{ow}$ of 3–4) and exposure times long enough to reach steady state, the steady-state SC permeability (P_{cv}) greatly overestimates dermal absorption, while the steady-state SC-EPI composite permeability (P_v) significantly underestimates dermal absorption.

A system of algebraic equations reasonably represents

unsteady-state absorption into the SC-EPI composite. During the unsteady-state period, the normalized cumulative mass entering the SC is the same for all chemicals and accurately represented by the semi-infinite membrane expression, Eq. (14). After the unsteady-state period, the cumulative mass entering the SC is predicted well with Eq. (20). This expression correctly represents the mass transfer restriction provided by the relatively hydrophilic EPI to the flux of highly lipophilic chemicals. The actual cumulative mass absorbed for a given chemical is calculated by multiplying the normalized cumulative mass by $(AK_{cv}L_cC_v^0)$. Consequently, the mass absorbed depends directly on the chemical concentration as well as its SC-vehicle partitioning. When experimentally determined values are not available, K_{cv} , D_c , and B are calculated a priori using expressions based on the SC permeability correlation and expectations of MW dependence for the EPI.

ACKNOWLEDGMENTS

This work was supported in part by the United States Environmental Protection Agency under Assistance Agreement No. CR817451. We thank R. H. Guy, R. O. Potts, and K. Hoang for their valuable suggestions and input.

NOMENCLATURE

A	Surface area of chemical exposure
b	Parameter in t^* calculation, Table I
B	SC-EPI permeability ratio; a parameter for the SC-EPI composite measuring the ratio of the SC permeability to the EPI permeability
c	Parameter in t^* calculation, Table I
C	Concentration
C_c	Concentration of the absorbing chemical in the SC
C_e	Concentration of the absorbing chemical in the EPI
C_v^0	Concentration of the absorbing chemical in the vehicle; assumed to remain constant during the exposure period, t_{exp}
D_c	Effective diffusivity of the absorbing chemical in the SC
D_e	Effective diffusivity of the absorbing chemical in the EPI
EPI	Viable epidermis
K_{ce}	Equilibrium partition coefficient between the SC and the EPI for the absorbing chemical
K_{cv}	Equilibrium partition coefficient between the SC and the vehicle for the absorbing chemical
K_{ev}	Equilibrium partition coefficient between the EPI and the vehicle for the absorbing chemical
K_{ow}	Octanol-water partition coefficient
L_c	Effective thickness of the SC
L_e	Effective thickness of the EPI
M	Cumulative mass transferring during an exposure period, t_{exp}
M^∞	Cumulative mass transferring during a very long exposure period, t_{exp}
M_{in}	Cumulative mass absorbed into the SC during an exposure period, t_{exp}
M_{out}	Cumulative mass leaving the SC during an exposure period, t_{exp}
MW	Molecular weight of the absorbing chemical

n	Summation index in Eqs. (9), (11), and (15)
P_{cv}	Steady-state permeability of the SC from a specified vehicle
P_{cw}	Steady-state permeability of the SC from water
P_{ev}	Steady-state permeability of the EPI from a specified vehicle
P_v	Steady-state permeability of the SC-EPI composite membrane from a specified vehicle
SC	Stratum corneum
t^*	Time to approximately reach steady state; expressions for estimating are given in Table I
t_{exp}	Time period of exposure event
t_{lag}	Lag time; time intercept of the finite, single-membrane long-exposure time equation [Eq. (13)]

Greek

τ Dimensionless exposure time defined by Eq. (10)

REFERENCES

- U.S. EPA. *Review of Dermal Absorption*, Office of Health and Environmental Assessment, Washington, DC, EPA/600/8-84/033, Oct. 1984.
- J. K. Hawley. Assessment of health risk from exposure to contaminated soil. *Risk Anal.* 5:289-301 (1985).
- E. A. Ryan, E. T. Hawkins, B. Magee, and S. L. Santos. Assessing risk from dermal exposure to hazardous waste sites. In: *Proc. 8th Natl. Conf., Superfund '87*, Washington, DC, Nov. 16-18, 1987, pp. 166-168.
- G. B. Kasting, R. L. Smith, and E. R. Cooper. Effect of lipid solubility and molecular size on percutaneous absorption. In B. Shroet and H. Schaefer (eds.), *Skin Pharmacokinetics*, Karger, Basel, 1987, pp. 138-153.
- G. L. Flynn. Physicochemical determinants of skin absorption. In Gerrity, T. R., and Henry, C. J. (eds.), *Principles of Route-to-Route Extrapolation for Risk Assessment*, Elsevier, New York, 1990, pp. 93-127.
- R. O. Potts and R. H. Guy. Predicting skin permeability. *Pharm. Res.* 9:663-669 (1992).
- R. J. Scheuplein. Mechanisms of percutaneous absorption. II. Transient diffusion and the relative importance of various routes of skin penetration. *J. Invest. Dermatol.* 48:79-88 (1967).
- W. J. Albery and J. Hadgraft. Percutaneous absorption: Theoretical description. *J. Pharm. Pharmacol.* 31:129-139 (1979).
- R. H. Guy and J. Hadgraft. A theoretical description relating skin penetration to the thickness of the applied medication. *Int. J. Pharm.* 6:321-332 (1980).
- R. H. Guy and J. Hadgraft. Physicochemical interpretation of the pharmacokinetics of percutaneous absorption. *J. Pharmacokin. Biopharm.* 11:189-203 (1983).
- P. H. Dugard. Absorption through the skin: Theory, in vitro techniques and their applications. *Food Chem. Toxicol.* 26:749-753 (1986).
- O. Siddiqui, M. S. Roberts, and A. E. Polack. Percutaneous absorption of steroids: Relative contributions of epidermal penetration and dermal clearance. *J. Pharmacokin. Biopharm.* 17:405-424 (1989).
- G. E. Parry, A. L. Bunge, G. D. Silcox, L. K. Pershing, and D. W. Pershing. Percutaneous absorption of benzoic acid across human skin. I. In vitro experiments and mathematical modeling. *Pharm. Res.* 7:230-236 (1990).
- G. D. Silcox, G. E. Parry, A. L. Bunge, L. K. Pershing, and D. W. Pershing. Percutaneous absorption of benzoic acid across human skin. II. Prediction of an in vivo skin flap system using in vitro parameters. *Pharm. Res.* 7:352-358 (1990).
- A. Rougie, M. Rallis, A. Krein, and C. Lotte. In vivo percutaneous absorption: A key role for stratum corneum vehicle partitioning. *Arch. Dermatol. Res.* 282:498-505 (1990).
- D. Southwell, B. W. Barry, and R. Woodford. Variations in

- permeability of human skin and between specimens. *Int. J. Pharm.* 18:299-309 (1984).
17. R. O. Potts. Private communication (1991).
 18. R. J. Scheuplein and I. H. Blank. Permeability of the skin. *Physiol. Rev.* 51:702-747 (1971).
 19. I. H. Blank and D. J. McAuliffe. Penetration of benzene through human skin. *J. Invest. Dermatol.* 85:522-526 (1985).
 20. J. Crank. *The Mathematics of Diffusion*, Oxford University Press, Oxford, 1975.
 21. H. S. Carslaw and J. C. Jaeger. *Conduction of Heat in Solids*, 2nd ed., Clarendon Press, Oxford, 1980.
 22. M. N. Ozisik. *Heat Conduction*, John Wiley & Sons, New York, 1980.
 23. A. L. Bunge and R. L. Cleek. *Dermal Absorption from Soils. 1. General Approach for Estimating Dermal Absorption from Chemical Exposure*, Report to U.S. Environmental Protection Agency, Assistance Agreement No. CR817451, submitted Aug. 1992.
 24. Bunge, A. L., G. L. Flynn, and R. H. Guy. A predictive model for dermal exposure assessment. In R. G. M. Wang (ed.), *Water Contamination and Health: Integration of Exposure Assessment, Toxicology, and Risk Assessment*, Ch. 15, Marcel Dekker, New York, 1992 (in press).
 25. R. J. Scheuplein. Molecular structure and diffusional processes across intact skin. Final report to the US Army Chemical R&D Laboratories, Edgewood Arsenal, MD, Contract DA 18-108-AMC-726(A) (1967).
 26. R. J. Scheuplein, I. H. Blank, G. J. Brauner, and D. J. MacFarlane. Percutaneous absorption of steroids. *J. Invest. Dermatol.* 52:63-70 (1969).
 27. M. S. Roberts, R. A. Anderson, D. E. Moore, and J. Swarbick. The distribution of nonelectrolytes between human stratum corneum and water. *Aust. J. Pharm. Sci.* 6:77-82 (1977).
 28. U.S. EPA. *Dermal Exposure Assessment: Principles and Applications*, Office of Health and Environmental Assessment, Washington, DC, EPA/600/8-91/011F, Jan. 1992.
 29. R. H. Guy and J. Hadgraft. Pharmacokinetic interpretation of the plasma levels of clonidine following transdermal delivery. *J. Pharm. Sci.* 74:1016-1018 (1985).
 30. A. L. Bunge and R. L. Cleek. A new method for estimating dermal absorption from chemical exposure. 2. Effect of molecular weight and octanol-water partitioning (submitted) (1992).
 31. J. A. Barrie, J. D. Levine, A. S. Michaels, and P. Wong. Diffusion and solution of gases in composite rubber membranes. *Trans. Faraday Soc.* 59:869-878 (1963).
 32. R. A. Siegel. Algebraic, differential, and integral relations for membranes in series and other multilaminar media: Permeabilities, solute consumption, lag times, and mean first passage times. *J. Phys. Chem.* 95:2556-2565 (1991).